

Thermo-optic coefficient of silicon at 1550 nm and cryogenic temperatures

Cite as: Appl. Phys. Lett. **101**, 041905 (2012); <https://doi.org/10.1063/1.4738989>

Submitted: 25 May 2012 • Accepted: 09 July 2012 • Published Online: 24 July 2012

J. Komma, C. Schwarz, G. Hofmann, et al.



View Online



Export Citation

ARTICLES YOU MAY BE INTERESTED IN

Temperature dependence of the thermo-optic coefficient in crystalline silicon between room temperature and 550 K at the wavelength of 1523 nm

Applied Physics Letters **74**, 3338 (1999); <https://doi.org/10.1063/1.123337>

Temperature dependence analysis of the thermo-optic effect in silicon by single and double oscillator models

Journal of Applied Physics **88**, 7115 (2000); <https://doi.org/10.1063/1.1328062>

Tutorial on narrow linewidth tunable semiconductor lasers using Si/III-V heterogeneous integration

APL Photonics **4**, 111101 (2019); <https://doi.org/10.1063/1.5124254>

Lock-in Amplifiers
up to 600 MHz



Zurich
Instruments



Thermo-optic coefficient of silicon at 1550 nm and cryogenic temperatures

J. Komma, C. Schwarz, G. Hofmann, D. Heinert, and R. Nawrodt^{a)}

Friedrich-Schiller-Universität Jena, Institut für Festkörperphysik, Helmholtzweg 5, D-07743 Jena, Germany

(Received 25 May 2012; accepted 9 July 2012; published online 24 July 2012)

The thermo-optic coefficient dn/dT of silicon was measured at 1550 nm in the wide temperature range from 5 K to 300 K. For this purpose an interferometric measurement scheme was applied using the silicon sample as a Fabry-Perot etalon. The high resolution of this setup revealed a thermo-optic coefficient as low as 10^{-8} K^{-1} at 5 K. The presented results show an excellent agreement with former measurements above 30 K including a value of $dn/dT = 1.8 \times 10^{-4} \text{ K}^{-1}$ at 300 K. © 2012 American Institute of Physics. [<http://dx.doi.org/10.1063/1.4738989>]

Silicon is widely used as an optical material in macroscopic and microscopic opto-mechanical applications. For transmissive optics its indirect band gap of around 1.12 eV prevents a use in the visible spectrum due to the high absorption with respect to interband transitions. However, operation in the near infrared band beyond about 1200 nm provides a sufficiently low optical absorption for high power applications. Powerful and highly stable lasers around 1550 nm used in fiber-optic communication make this wavelength a good candidate for the use of silicon optics. Additionally, the low mechanical loss of silicon at cryogenic temperatures^{1,2} suggests its use in low thermal noise experiments such as gravitational wave detectors^{3,4} or cavities used for laser frequency stabilization.⁵

Applications using optical components at high laser powers can suffer from thermal lensing effects. If light gets absorbed a spatial temperature distribution within the sample is created due to the intensity profile of the laser beam. By means of the thermo-optic coefficient $\beta = dn/dT$ this temperature profile creates a refractive index profile and thus a lens type element. This thermal lens may affect the optical function of a setup significantly and can even degrade the performance dramatically.

Further, statistical temperature fluctuations in optical components will cause changes of the refractive index and thus phase fluctuations by means of the thermo-optic coefficient. This thermo-refractive noise⁶ can play an important role in limiting the sensitivity of high-precision opto-mechanical measurements.⁷ Besides the mentioned macroscopic metrological applications silicon is also a candidate material for microscopic applications such as whispering gallery resonators.^{8,9} With their sharp optical spectra these devices promise advantages in the fields of spectroscopy and sensing. Thermo-refractive noise was also identified to strongly limit the scope of these microscopic resonators.¹⁰

A possible solution to overcome these limitations—both thermal lensing and thermo-refractive noise—is cooling the optical components to cryogenic temperatures. Unfortunately, the thermo-optic coefficient is just reported to temperatures down to 30 K (Ref. 11) while most possible applications are operating or proposed to operate at temperatures below that.

In this letter a measurement for the thermo-optic coefficient β of silicon in the temperature region of 5 K to 300 K is presented. The interferometric scheme proposed by Cocorullo *et al.*¹² was adapted to cryogenic temperatures allowing a precise measurement of dn/dT with an uncertainty of $2 \times 10^{-8} \text{ K}^{-1}$ at 5 K. Finally, the results for silicon are compared to fused silica as a widely-used material in optical applications.

The basic idea of the measurement principle can be illustrated by a simple Fabry-Perot Cavity (FPC). For a symmetric cavity with two equal mirrors the reflected intensity is given by

$$I_R = \frac{I_0}{1 + 1/(F \sin^2 \Theta)}, \quad (1)$$

where I_0 is the incident light intensity and Θ is the phase change for a single pass at normal incidence given by

$$\Theta = 2\pi nL/\lambda. \quad (2)$$

Here L describes the geometric distance between the mirrors, n the refractive index of the medium between them and λ the wavelength of the incident light. The finesse coefficient F of the cavity is determined by

$$F = \frac{4R}{(1 - R)^2}, \quad (3)$$

with the reflectance R of the mirrors.

The experiment presented in this letter uses a silicon etalon instead of a cavity. In this setup the Fresnel reflections at the surface form the mirrors of an FPC. Due to its high refractive index of 3.48 at 1550 nm a reflectance of about 31% is achieved at each interface.

A change in the sample temperature leads to a change of the optical path of the light passing through the sample due to both, a change in the refractive index n as well as in the geometrical length, L , via the coefficient of thermal expansion, α . This phase change is transferred into an intensity change by means of Eq. (1). Fig. 1 exemplarily shows the measured behavior within a 5 K interval around room temperature.

The sample was cut from a silicon single crystal substrate to a size of approximately $5 \text{ mm} \times 6 \text{ mm} \times 14 \text{ mm}$. Both $5 \text{ mm} \times 6 \text{ mm}$ faces were flat lapped and polished to an

^{a)}Electronic mail: ronny.nawrodt@uni-jena.de.

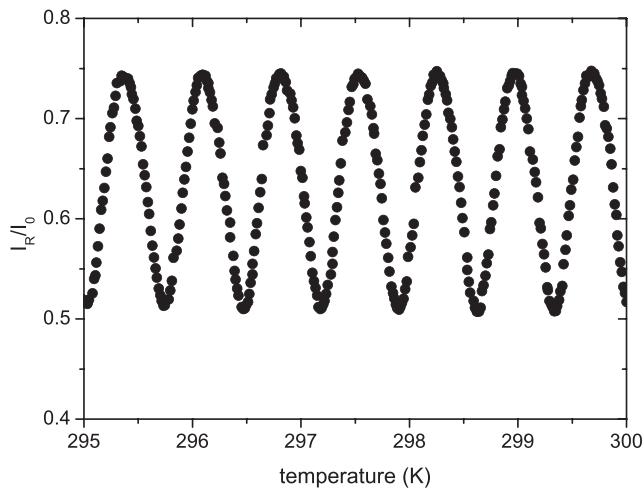


FIG. 1. Measured intensity change of the light reflected from a 6 mm long silicon Fabry-Perot etalon due to a temperature change from 295 K to 300 K. The reflected intensity I_R was normalized to the incoming light power I_0 .

optical quality after cutting. These two polished faces form the end mirrors of the etalon and need to be very well aligned in order to minimize lateral reflections that do not contribute to the interference and thus reduce the signal modulation depth.

The boron doping level of the samples was of the order of 10^{16} cm^{-3} . This leads to a typical optical absorption coefficient below 0.1 cm^{-1} at room temperature which was confirmed experimentally. At low temperatures the optical absorption of silicon is expected to be very small and thus can be neglected during the data evaluation presented here. Any optical absorption below 1 cm^{-1} is tolerable for the presented measurement scheme due to the cooling capacity of the cryostat.

A liquid helium flow cryostat was used to provide sample temperatures between 4 K and 300 K. The lowest temperature was reached within less than one hour due to the small thermal load. The cryostat is capable of hosting samples with a longest dimension of up to 16 mm. Fig. 2 shows a schematic sketch of the setup: The sample (1) is placed in the probe chamber (2) inside the cryostat (3). To cool down the sample 1 mbar of helium gas was applied to the inner vacuum chamber to guarantee sufficient thermal contact during the cooling process. At minimum temperature the probe

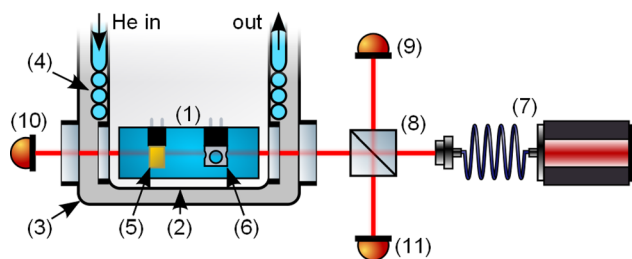


FIG. 2. Inside the continuous helium flow cryostat the sample (1) is placed in the probe chamber (2) which is surrounded by vacuum in the cryostat (3) to provide a thermal insulation against room temperature. A cooling coil (4) allows the heat extraction by an adjustable liquid helium flow. Directly attached to the sample is a calibrated temperature sensor (5) as well as an electric heater (6). The beam from the 1550 nm laser source (7) is split (8) into two parts. One of them is detected by a reference photo diode (9) and the other one points in the direction of the sample. Two additional photo diodes measure the transmitted (10) and the reflected (11) light intensity.

volume was evacuated to thermally decouple the sample from the probe chamber.

A calibrated Lakeshore silicon diode temperature sensor type DT670 (5) was mounted directly on the sample for a precise temperature measurement with an accuracy of at least 50 mK throughout the whole temperature range. An electric heater (6) also placed on the sample allowed a closed loop setting of absolute temperatures as well as constant cooling or heating rates at the sample. A Lakeshore temperature controller LS336 was used to control the sample temperature and the cooling as well as the heating rates. Typical rates were in the order of 2 K/min to 8 K/min depending on the temperature range. Independent measurements at different temperature rates guaranteed reproducible results. This confirms that the rates used allowed an effective thermalisation of the sample at all temperatures.

While the temperature of the sample is changed by the closed loop heating system the windows of the cryostat were kept at a constant low temperature. A variation in the window temperature would lead to a beat-like modulation of the fringe amplitudes from the silicon etalon and a more complicated data analysis. To minimize this effect sapphire windows were used. These windows were thermally connected to the cold part of the cryostat. Due to the high thermal conductivity of sapphire a homogenous temperature distribution across the free aperture is achieved. The window temperature was monitored with a separate temperature sensor. As the thermo-refractive coefficient of sapphire is smaller than $9 \times 10^{-8} \text{ K}^{-1}$ at temperatures below 40 K (Ref. 13) the effect of the windows onto the final results is negligible.

The light source was realized by an adjustable Er-fibre laser (7) model AQ2200-136 TLS made by Yokogawa. It provides a tunable wavelength between 1440 nm and 1640 nm and a maximum output power of about 20 mW. Using a non-polarizing beam splitter (8) a fraction of the incident light was directed onto a photo diode (9). Its signal was used for normalization of the reflected and transmitted power. Typical laser powers at the location of the test sample were in the order of 5–10 mW. The transmitted as well as the reflected light were measured by two additional photo diodes (10) and (11). The laser power was sensed with a resolution better than $1 \mu\text{W}$ at each photo diode.

The temperature derivation of the phase term given in Eq. (2) is

$$\frac{\delta\Theta}{\delta T} = \frac{2\pi}{\lambda} \left(L \frac{\delta n}{\delta T} + n \frac{\delta L}{\delta T} \right) = \frac{2\pi L}{\lambda} \left(\frac{\delta n}{\delta T} + n(T) \alpha(T) \right). \quad (4)$$

This allows the discrete calculation of the thermo-optic coefficient β . The phase change between two neighboring intensity maxima equals π . With the temperature difference ΔT between these maxima the thermo-optic parameter follows

$$\beta(T) = \frac{\delta n}{\delta T} = \frac{\lambda}{2L\Delta T} - n(T) \alpha(T). \quad (5)$$

The evaluation of Eq. (5) was started at room temperature with literature values for the refractive index¹¹ n , the coefficient of thermal expansion¹⁴ α and the measured sample length L . The iterative evaluation was applied at temperatures above 26 K. This allows a sufficiently high density of

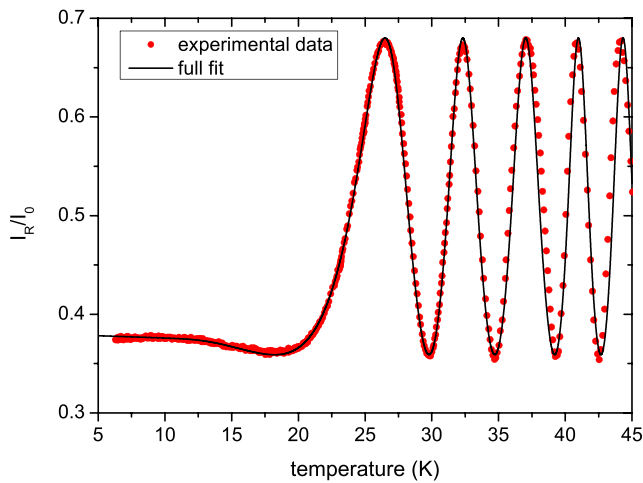


FIG. 3. Fit of the low temperature data used to extract the thermo-optic coefficient (red dots) underlying the extraction of the thermo-optic parameter of silicon. The reflected intensity was normalized using the incoming laser power I_0 .

data points for the thermo-optic coefficient. Below 26 K the coefficient of thermal expansion as well as the change in the refractive index become very small. Thus, with decreasing the temperature a full phase shift of π cannot be reached again and the evaluation strategy needs to be changed. As the measured values are changing slowly with temperature a full fit of the data observed was done using Eqs. (1) and (4) (see Fig. 3).

The results are given in Fig. 4 between 5 K and 300 K for the sample of 14 mm in length. Different measurements have been performed with different sample lengths, and all gave the same results. In the temperature range from 30 K to 300 K an excellent agreement with existing literature values¹¹ exists. Below 30 K the thermo-optic coefficient continuously decreases and reaches a value as low as 10^{-8} K^{-1} at 5 K. This continuous decrease of the temperature dependence of the refractive index is in agreement with the third law of thermodynamics which states that all temperature dependent parameters have to become constant going towards 0 K.

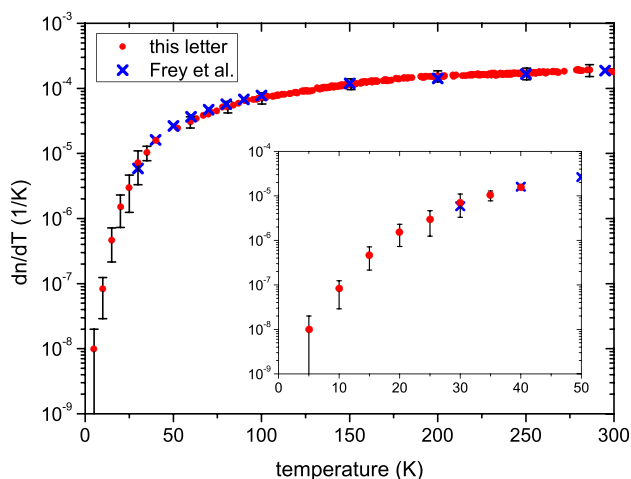


FIG. 4. Results for the thermo-optic coefficient of silicon at 1550 nm in the temperature range from 5 K to 300 K. The inset gives a detailed overview of the low temperature part of the curve. The comparison with values obtained by Frey *et al.*¹¹ reveals an excellent agreement.

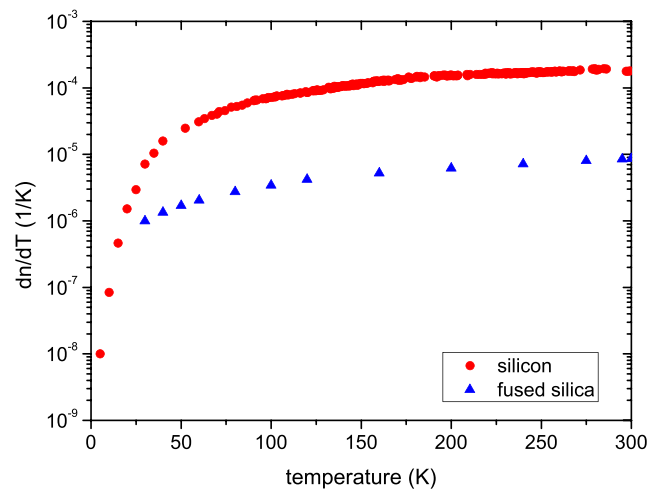


FIG. 5. Comparison of the thermo-optic coefficient of fused silica (Corning 7980, see Ref. 16) and silicon as a function of temperature.

At high temperatures the main limitation of the measurement is due to the uncertainty in the determination of the temperature difference between two intensity maxima. In contrast, the low temperature range is limited by the resolution of the intensity measurement and thus the accuracy of the fit.

In Fig. 5 the presented results for silicon are compared to fused silica that is widely used in high power optics due to its low optical absorption.¹⁵ At room temperature silica provides a low thermo-optic coefficient¹⁶ of $8.5 \times 10^{-6} \text{ K}^{-1}$.

The respective value of silicon is more than one order of magnitude larger. In applications demanding low thermal noise, cooling of the substrates represents a way to further reduce the noise. But at low temperatures the high mechanical loss¹⁷ in fused silica precludes its use as a substrate material due to the increased Brownian thermal noise.³ In contrast, silicon promises an effective noise reduction below 30 K as it shows a low mechanical loss and its thermo-optic coefficient drops below the room temperature value of fused silica.

Additionally, in the low temperature regime crystalline silicon exhibits a higher thermal conductivity compared to amorphous fused silica. This property prevents the appearance of strong temperature gradients in the sample and so further reduces the effect of thermal lensing.

The use of our interferometric measurement setup allowed the accurate measurement of the thermo-optic coefficient in silicon. At 1550 nm a minimum value as low as 10^{-8} K^{-1} around 5 K was observed. A comparison with fused silica, a widely used optical material, highlights the advantage of silicon at temperatures below 30 K. In this region the effect of thermal lensing as well as the driving terms for thermo-refractive noise are expected to be smaller for silicon. Thus, together with its low mechanical loss silicon is an ideal material for high intensity and low noise optics. This makes it of interest for cavity based laser stabilization, quantum measurements (e.g., entanglement) or interferometric gravitational wave detectors.

This work was supported by the German science foundation under Contract No. SFB TR7. The authors would like to acknowledge useful discussions with their colleagues of the Einstein Telescope Design Study.

- ¹D. F. McGuigan, C. C. Lam, R. Q. Gram, A. W. Hoffman, D. H. Douglas, and H. W. Gutche, *J. Low Temp. Phys.* **30**, 621 (1978).
- ²S. Rowan, J. Hough, and D. R. M. Crooks, *Phys. Lett. A* **347**, 25 (2005).
- ³R. Nawrodt, S. Rowan, J. Hough, M. Punturo, F. Ricci, and J.-Y. Vinet, *Gen. Relativ. Gravit.* **43**, 593 (2011).
- ⁴S. Hild, M. Abernathy, F. Acernese, P. Amaro-Seoane, N. Andersson, K. Arun, F. Barone, B. Barr, M. Barsuglia, M. Beker *et al.*, *Class. Quantum Grav.* **28**, 094013 (2011).
- ⁵J. P. Richard and J. J. Hamilton, *Rev. Sci. Instrum.* **62**, 2375 (1991).
- ⁶V. B. Braginsky, M. L. Gorodetsky, and S. P. Vyatchanin, *Phys. Lett. A* **271**, 303 (2000).
- ⁷D. Heinert, A. G. Gurkovsky, R. Nawrodt, S. P. Vyatchanin, and K. Yamamoto, *Phys. Rev. D* **84**, 062001 (2011).
- ⁸M. Borselli, K. Srinivasan, P. E. Barclay, and O. Painter, *Appl. Phys. Lett.* **85**, 3693 (2004).
- ⁹M. Ghulinyan, D. Navarro-Urrios, A. Pitanti, A. Lui, G. Pucker, and L. Pavesi, *Opt. Express* **16**, 13218 (2008).
- ¹⁰A. B. Matsko, A. A. Savchenkov, N. Yu, and L. Maleki, *J. Opt. Soc. Am. B* **24**, 1324 (2007).
- ¹¹B. J. Frey, D. B. Leviton, and T. J. Madison, e-print arXiv:physics/0606168v1.
- ¹²G. Cocorullo, F. G. D. Corte, and I. Rendina, *Appl. Phys. Lett.* **74**, 3338 (1999).
- ¹³T. Tomaru, T. Suzuki, S. Miyoki, T. Uchiyama, C. T. Taylor, A. Yamamoto, T. Shintomi, M. Ohashi, and K. Kuroda, *Class. Quantum Grav.* **19**, 20452049 (2002).
- ¹⁴K. G. Lyon, G. L. Salinger, C. A. Swenson, and G. K. White, *J. Appl. Phys.* **48**, 865 (1977).
- ¹⁵S. Hild, H. Lück, W. Winkler, K. Strain, H. Grote, J. Smith, M. Malec, M. Hewitson, B. Willke, J. Hough, and K. Danzmann, *Appl. Opt.* **45**, 7269 (2006).
- ¹⁶D. B. Leviton and B. J. Frey, e-print arXiv:0805.0091v1.
- ¹⁷O. L. Anderson and H. E. Bömmel, *J. Am. Ceram. Soc.* **38**, 125 (1955).